THE JOURNAL OF BIOLOGICAL CHEMISTRY
Vol. 275, No. 39, Issue of September 29, pp. 30668–30676, 2000

Printed in U.S.A.

Regulation of Brain Fatty Acid-binding Protein Expression by Differential Phosphorylation of Nuclear Factor I in Malignant Glioma Cell Lines*

Received for publication, May 5, 2000, and in revised form, June 23, 2000
Published, JBC Papers in Press, July 13, 2000, DOI 10.1074/jbc.M003828200

Dwayne A. Bisgrove‡, Elizabeth A. Monckton, Mary Packer, and Roseline Godbout§

From the Department of Oncology, Cross Cancer Institute and University of Alberta, 11560 University Avenue, Edmonton, Alberta T6G 1Z2, Canada

Brain fatty acid-binding protein (B-FABP) is expressed in the radial glial cells of the developing central nervous system as well as in a subset of human malignant glioma cell lines. Most of the malignant glioma lines that express B-FABP also express GFAP, an intermediate filament protein found in mature astrocytes. We are studying the regulation of the *B-FABP* gene to determine the basis for its differential expression in malignant glioma lines. By DNase I footprinting, we have identified five DNA-binding sites located within 400 base pairs (bp) of the *B-FABP* transcription start site, including two nuclear factor I (NFI)-binding sites at −35 to −58 bp (footprint 1, fp1) and −237 to −260 bp (fp3), respectively. Competition experiments, supershift experiments with anti-NFI antibody, and methylation interference experiments all indicate that the factor binding to fp1 and fp3 is NFI. By site-directed mutagenesis of both NFI-binding sites, we show that the most proximal NFI site is essential for *B-FABP* promoter activity in transiently transfected malignant glioma cells. Different band shift patterns are observed with nuclear extracts from B-FABP(+) and B-FABP(−) malignant glioma lines, with the latter generating complexes that migrate more slowly than those obtained with B-FABP(+) extracts. All bands are converted to a faster migrating form with potato acid phosphatase treatment, indicating that NFI is differentially phosphorylated in B-FABP(+) and B-FABP(−) lines. Our results suggest that B-FABP expression in malignant glioma lines is determined by the extent of NFI phosphorylation which, in turn, is controlled by a phosphatase activity specific to B-FABP(+) lines.

Malignant gliomas are believed to be derived from the astrocytic cell lineage because they contain bundles of cytoplasmic glial fibrillary acidic protein (GFAP),[1] an intermediate filament protein specifically expressed in differentiated astrocytes. There is an inverse relationship between the number of GFAP-positive cells and aggressive behavior in glioma tumors. Glioblastoma multiforme, the most common and aggressive glioma, often have low GFAP expression, while low grade astrocytomas usually have high levels of GFAP (1–4). *In vitro* studies directly correlate GFAP expression with a less aggressive behavior (5). Transfection of a GFAP expression vector into GFAP(−) malignant glioma cells results in decreased cell proliferation and decreased growth in soft agar (6, 7). Conversely, transfection of a GFAP antisense vector into a GFAP(+) line results in undetectable GFAP expression and increased proliferation rate, anchorage-independent growth, and invasiveness (8).

We have previously shown that GFAP(+) malignant glioma lines express a second glial cell marker, brain fatty acid-binding protein (B-FABP) (9). Of 15 malignant glioma lines tested, 5 co-expressed B-FABP and GFAP, 8 expressed neither gene, while 2 had low levels of B-FABP and undetectable levels of GFAP. B-FABP is a 15-kDa protein normally found in the radial glial cells of the developing central nervous system as well as in select glial cell populations of the adult brain including glia limitans cells and Bergmann glial cells (10, 11). B-FABP expression has been implicated in the establishment of the radial glial fiber system which serves to guide immature migrating neurons to their correct location in the central nervous system (10, 12). Addition of anti-B-FABP antibody to primary cultures of cerebellar cells prevents both the extension of radial glial processes and the migration of neuronal cells along these processes, suggesting a role for B-FABP in relaying inductive signals required for glial cell differentiation.

It is generally believed that radial glial cells are converted into astrocytes once neuronal migration in the developing brain is complete (13). Co-expression of GFAP and B-FABP in the same malignant glioma cells (9) therefore suggests that these tumors are derived from cells that have the potential of expressing proteins that are normally produced at different stages in the glial differentiation pathway. We are studying the regulation of the *B-FABP* gene in order to identify transcription factors involved in the regulation of glial genes in malignant glioma and understand the basis for the variation in B-FABP expression in different malignant glioma lines. By sequencing and DNase I footprinting, we have identified two NFI-binding sites in the promoter region of the *B-FABP* gene. We present evidence that a phosphatase specifically expressed in B-FABP(+) cells is responsible for differential expression of the *B-FABP* gene in malignant glioma lines.

* This work was supported in part by a Research Initiative Program grant from the Alberta Cancer Board and the Alberta Cancer Foundation. The costs of publication of this article were defrayed in part by the payment of page charges. This article must therefore be hereby marked "*advertisement*" in accordance with 18 U.S.C. Section 1734 solely to indicate this fact.

‡ Supported in part by a studentship from the Alberta Cancer Foundation.

§ To whom correspondence should be addressed: Dept. of Oncology, Cross Cancer Institute, 11560 University Ave., Edmonton, Alberta T6G 1Z2, Canada. Tel.: 780-432-8901; Fax: 780-432-8892; E-mail: rgodbout@gpu.srv.ualberta.ca.

[1] The abbreviations used are: GFAP, glial fibrillary acidic protein; B-FABP, brain fatty acid-binding protein; NFI, nuclear factor 1; PAP, potato acid phosphatase; kb, kilobase(s); bp, base pair(s); CAT, chloramphenicol acetyltransferase; MES, 4-morpholineethanesulfonic acid; fp1, footprinting region 1.

MATERIALS AND METHODS

Cloning the Human B-FABP Promoter—Isolation of the human *B-FABP* gene has been previously described (9). A 3-kb *Eco*RI fragment containing exons I, II, and 1.8 kb of 5′-flanking DNA was subcloned into pBluescript and sequenced. The *B-FABP* transcription start site was mapped by primer extension using primer 5′-CTCTTTAGAGACAGGAGCGGGGATC-3′ located at position +43 to +67 bp in the 5′-untranslated region.

Transfection of Malignant Glioma Cell Lines—A series of constructs with different amounts of 5′-flanking DNA (1.8 kb, 1.2 kb, 660 bp, 240 bp, and 140 bp) were linked to the chloramphenicol acetyltransferase (CAT) reporter gene and introduced into the U251 malignant glioma line by calcium phosphate-mediated DNA transfection. Cells were harvested 60 h after transfection and CAT activity measured using the protocol supplied by Promega. To control for plate to plate variation in transfection efficiency, Hirt DNA was isolated and quantitated by densitometric scanning of Southern blots (14). Samples generating a greater than 2-fold variation in transfection efficiency based on Hirt DNA analysis were discarded.

Site-directed mutagenesis of the fp1 and fp3 NFI DNA-binding sites was carried out by the method of Hemsley *et al.* (15). To introduce mutations in the fp1 NFI-binding site, inverse polymerase chain reaction was performed on pCAT-240 using *pfu* polymerase (Stratagene) and the head-to-head mutagenic primer set 5′-ATCAC**TAAA**TTTTT**GCCCA**CCCTC-3′ and 5′-TTAAATTGCAAACACACCCC-3′ (the NFI-binding site is in bold, underlined nucleotides represent the GG to AA mutation). After gel purification and recircularization, mutagenesis of the NFI-binding site was confirmed by automated sequencing (ABI Prism 310). A 190-bp *Xho*I/*Xba*I fragment containing the mutagenized fp1 NFI-binding site was exchanged for the corresponding wild type fragment in pCAT-1.8 to generate pCAT1.8(fp1*). To introduce mutations in the fp3 NFI-binding site (pCAT-1.8(fp3*)), we used mutagenic primers 5′-AGCCCCAT**AAAA**TCCCT**GCCGA**G-3′ and 5′-GGAGGCAGGGAACGGGAAAATGAG-3′. The double mutant construct (pCAT-1.8(fp1*3*)) combines both the fp1 and fp3 mutations and was obtained by replacing the 1629-bp wild type *Eco*RI/*Xho*I fragment of pCAT1.8(fp1*) with the corresponding region of pCAT-1.8(fp3*).

DNase I Footprinting Analysis—DNA probes labeled at one end were produced by linearizing plasmids containing either a 228-bp *Alu*I fragment (−13 to −240 bp) or a 281-bp *Eco*O109I/*Xho*I fragment (−138 to −418 bp) with *Xba*I or *Hin*dIII (enzymes that cut in the polylinker region), respectively, and filling-in with Klenow polymerase in the presence of [α-^{32}P]dCTP. Radiolabeled DNA fragments were released by digesting with either *Hin*dIII or *Xba*I, respectively, and purifying the DNA by gel electrophoresis and electroelution. The G + A chemical sequencing reaction was according to Belikov and Wieslander (16). Nuclear extracts were prepared from malignant glioma cell lines as described (17).

DNase I footprinting was carried out as described previously except that polyvinyl alcohol was omitted from the binding buffer (18). Briefly, radiolabeled DNA probe (10 fmol) was incubated with the indicated malignant glioma nuclear extracts (20 μg) in binding buffer for 15 min on ice, followed by 2 min at room temperature. An equal volume of 5 mM $CaCl_2$, 10 mM $MgCl_2$ was added, followed by DNase I (Worthington, DPFF code) to 1 μg/ml. The samples were digested for 1 min and the reaction stopped with 0.2 M NaCl, 20 mM EDTA, 1% SDS. The DNA was purified by phenol/chloroform extraction and ethanol precipitation. Samples were resuspended in formamide loading buffer and denatured at 90 °C for 3 min prior to electrophoresis through an 8% polyacrylamide denaturing gel.

Gel Shift Assay—The gel shift assay was carried out as described by O'Brien *et al*. (19). Complementary oligonucleotides (Scheme I) were annealed and radiolabeled by filling-in with Klenow polymerase in the presence of [α-^{32}P]dCTP or [α-^{32}P]dATP. Nuclear extracts (4 μg) were preincubated with 2 μg of poly(dI-dC) in binding buffer (20 mM HEPES, pH 7.9, 20 mM KCl, 1 mM spermidine, 10 mM dithiothreitol, 10% glycerol, 0.1% Nonidet P-40) for 10 min at room temperature. When included, a 100-fold excess of unlabeled competitor oligonucleotide was added during the preincubation stage. AP-2, CTF/NFI, and Sp1 oligonucleotides were purchased from Promega. For supershift experiments, 2 μl of either anti-NFI antibody (rabbit polyclonal antiserum shown to react with the C-terminal half of NFI, obtained from Dr. Naoko Tanese, NYU Medical Center, NY) or anti-AP-2 antibody (Santa Cruz Biotechnology) was included in the binding reaction. Labeled probe DNA (25 fmol) was added and incubated for 20 min at room temperature. DNA-protein complexes were resolved on a 6% polyacrylamide gel in 0.5 × TBE.

Dephosphorylation of nuclear extracts using potato acid phosphatase (PAP) was carried out by incubating 4 μg of T98 or U251 nuclear extracts with the indicated amount of PAP (Sigma) in 0.1 M MES buffer (pH 6.0) at room temperature for 30 min. To detect endogenous phosphatase activity, nuclear extracts were dialyzed in phosphate-free buffer (25 mM HEPES, pH 7.6, 40 mM KCl, 0.1 mM EDTA, 1 mM dithiothreitol, 10% glycerol, and 0.2 mM phenylmethylsulfonyl fluoride) and incubated at 30 °C for 30 min prior to the gel shift assay. Where indicated, 50 mM K_2PO_4, pH 7.4, was added as a phosphatase inhibitor.

Methylation Interference Assay—The protein-DNA binding reaction (described under "Gel Shift Assay") was scaled up 5-fold using partially methylated fp1 oligonucleotide probe labeled on either the coding or non-coding strands. DNA methylation and methylation interference assay were as described by Garabedian *et al.* (20). Briefly, bound and free DNA were excised from the mobility shift gel, eluted overnight in 0.2 M NaCl, 20 mM EDTA, 1% SDS, 1 mg/ml yeast tRNA, and purified by phenol/chloroform extraction and ethanol precipitation. Eluted DNA was cleaved with piperidine at 90 °C for 30 min and residual piperidine removed by lyophilization. The DNA was resuspended in formamide loading buffer, denatured at 90 °C for 3 min, and resolved on a 12% polyacrylamide denaturing gel.

Western Blot Analysis—Nuclear extracts (25 μg) prepared from B-FABP(+) and B-FABP(−) malignant glioma lines were electrophoresed through an 8% polyacrylamide-SDS gel followed by electroblotting onto nitrocellulose. For the dephosphorylation experiments, nuclear extracts (20 μg) from either U251 or T98 were treated with PAP in 0.1 M MES, pH 6.0, for 20 min at 30 °C. Filters were incubated with a 1/1000 dilution of anti-NFI antibody and the primary antibody detected with horseradish peroxidase-conjugated anti-rabbit IgG (Jackson ImmunoResearch Laboratories) using the ECL detection system (Amersham Pharmacia Biotech).

RESULTS

Analysis of the B-FABP Promoter Region—We have previously shown that the human *B-FABP* gene is contained within a 4.5-kb region on chromosome 6q22–23 (9). To study the regulation of *B-FABP* transcription, we first mapped the transcription initiation site by primer extension. The human *B-FABP* gene start site is located 81 bp upstream of the translation initiation codon (data not shown) within three nucleotides of that reported for murine *B-FABP* (11, 21). There is a putative TATA box (AATAAGA) at position −22 to −28 bp (Fig. 3).

To determine the location of *B-FABP* regulatory elements in malignant glioma, we tested CAT reporter constructs containing different amounts of *B-FABP* 5′-flanking DNA (Fig. 1*A*). These constructs were introduced into U251, a malignant glioma line that expresses B-FABP. As shown in Fig. 1*B*, a 2-fold increase in CAT activity was observed with 240 bp of 5′-flanking DNA (pCAT-240). Additional 5′-flanking DNA, to −660 and −1800 bp produced 6- and 8-fold increases in basal CAT activity, respectively. These results indicate that there are multiple positive regulatory elements in the −140 to −1800-bp region of the *B-FABP* gene.

DNase I Footprint Analysis of the B-FABP Promoter—To identify DNA-protein interaction sites proximal to the *B-FABP* gene, we carried out DNase I footprinting analysis using two overlapping DNA fragments spanning the region from −13 to −418 bp: probe 1, from −13 to −240 bp, and probe 2, from −138 to −418 bp. Probe 1 or probe 2, labeled at one end, were incubated with nuclear extracts from both B-FABP(+) (M016, U251) and B-FABP(−) (T98) malignant glioma lines and partially digested with DNase I followed by denaturing gel electrophoresis and autoradiography. As shown in Fig. 2*A*, two DNase I protected regions were detected using probe 1: footprint 1 (fp1) from −35 to −58 bp and fp2 from −155 to −174 bp. Probe 2 identified three additional protected regions, from −237 to −260 bp (fp3), −303 to −328 bp (fp4), and −340 to −359 bp (fp5) (Fig. 2*B*). Identical results were obtained with both B-FABP-positive and -negative nuclear extracts. These data are summarized in Fig. 3.

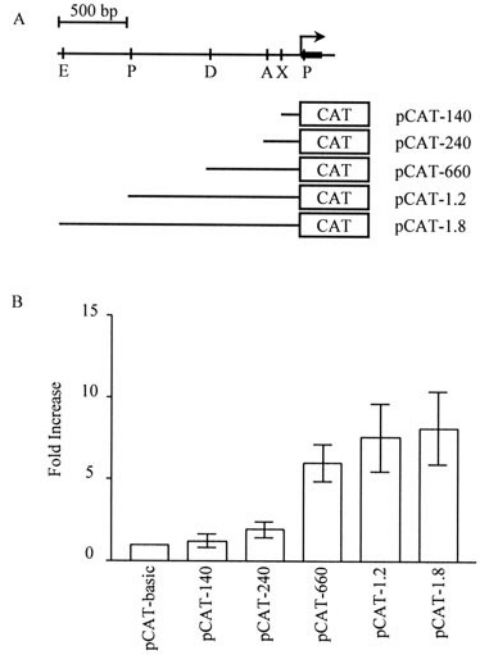

FIG. 1. **Analysis of the *B-FABP* upstream region for regulatory activity.** *A,* schematic diagram of the *B-FABP* promoter showing the transcription start site (*arrow*), exon I (*filled box*), and restriction enzyme sites used for the construction of the pCAT-deletion plasmids. The B-FABP-CAT constructs extend from a common 3′ *Pst*I (P) site to various upstream sites (at −140, −240, −660 bp, −1.2 and −1.8 kb) generated by restriction enzyme digestion. *B,* 10 μg of each of the B-FABP-CAT constructs described above were introduced into U251 by calcium phosphate-mediated DNA transfection. Extracts prepared from transfected cells were assayed for CAT activity by monitoring the level of [^{14}C]chloramphenicol butyrylation. CAT activity is reported as fold increase over the promoter-less parent vector pCAT-basic. The values have been normalized for transfection efficiency by Hirt DNA quantitation. The results shown are an average of at least four independent experiments with standard deviation indicated by the *error bars*.

The sequences of the five footprints were analyzed using the Transfac program (22) and by visual inspection to identify known DNA binding motifs. Fp1, fp2, and fp3 all contained putative NFI-binding sites based on similarity to the NFI consensus binding site TGGA/C(N_5)GCCAA (23–25). The fp1 region contained the sequence TGGA(N_5)GCCCA, fp2 TGGC(N_4)GCCAA, and fp3 TGAA(N_5)GCCGA.

Protein Binding to Fp1 and Fp3—We used the mobility shift assay to determine whether a double-stranded oligonucleotide with a consensus NFI-binding site could effectively compete for protein binding to either fp1 or fp3. Radiolabeled oligonucleotides corresponding to fp1 or fp3 were incubated with extracts from either B-FABP(−) T98 cells or B-FABP(+) U251 cells, along with a 100-fold excess of unlabeled fp1, fp2, fp3, AP-2, NFI, or Sp1 oligonucleotides. One major DNA-protein complex was observed with T98 nuclear extract using either the fp1 or fp3 probes (Fig. 4). This complex was specifically competed out by fp1, fp3, and consensus NFI oligonucleotides, indicating that the factor bound to fp1 and fp3 is NFI or NFI-like. The inability of fp1, fp3, and NFI oligonucleotides to compete with fp2 indicates that fp2 does not represent a bona fide NFI-binding site, as suggested by the N-4 (as opposed to the N-5) spacing between the NFI half-sites. In contrast to T98, three major shifted complexes were detected with B-FABP(+) U251 nuclear extracts using either fp1 or fp3 as the probe. The intensity of all three bands was reduced upon addition of excess unlabeled fp1, fp3, and NFI oligonucleotides. These data suggest that, while generating different gel shift patterns, NFI or NFI-related proteins bind to the fp1 and fp3 regions of *B-FABP* promoter in both B-FABP(+) and B-FABP(−) malignant glioma lines.

Antibody supershift experiments were carried out to determine whether the factor(s) bound to the fp1 region was recognized by a pan-specific anti-NFI antibody. Nuclear extract from B-FABP(−) T98, B-FABP(+) U251, or B-FABP(+) M016 was incubated with anti-NFI antibody prior to the addition of labeled fp1 oligonucleotide. A supershifted band (indicated by the *arrow* in Fig. 5) was observed with all three extracts. Of note, the intensity of the protein-DNA complexes was greatly reduced upon addition of anti-NFI antibody suggesting disruption of the complex upon binding of the antibody. No supershifted band or reduction in band intensity was observed with control anti-AP-2 antibody.

The methylation interference assay was used to identify the purine residues in fp1 involved in DNA-protein interaction. Partially methylated fp1 oligonucleotide, radiolabeled on either the coding or non-coding strand, was isolated from the most abundant T98 gel shift complex and from the three major U251 complexes, and subjected to piperidine cleavage followed by denaturing polyacrylamide gel electrophoresis. As shown in Fig. 6, methylation of G residues located at −52, −51, and −44 bp on the coding strand, and −43 and −42 bp on the non-coding strand interfered with the formation of the T98 and U251 DNA-protein complexes. Identical methylation interference patterns were obtained for both T98 (B) and U251 (B1, B2, and B3) complexes, indicating that the same or a similar recognition sequence is involved in their formation. The observed methylation interference pattern is consistent with that of several known NFI-binding sites (26, 27). Together, the competition assays, supershift experiments and methylation interference experiments indicate that the NFI factor binds to the fp1 and fp3 regions.

Mutation Analysis of Fp1 and Fp3—To assess the biological role of the fp1 and fp3 NFI-binding sites, we transfected U251 with pCAT-1.8 constructs containing mutations in one or both NFI core recognition sequences. The mutations introduced in fp1 (pCAT-1.8(fp1*)), fp3 (pCAT-1.8(fp3*)), or both fp1 and fp3 (pCAT-1.8(fp1*fp3*)) are indicated in Scheme I. We first verified that the introduced mutations would eliminate DNA-protein interaction using the gel shift assay. As shown in Fig. 7*A*, mutant fp1* was unable to compete with normal fp1 for the formation of T98 and U251 DNA-protein complexes. Similar results were obtained with mutated fp3*.

When introduced into U251 cells, the parent construct pCAT-1.8 produced an 8-fold increase in CAT activity compared with the pCAT-basic construct (Fig. 7*B*). Mutation of the fp1 NFI-binding site reduced transcriptional activity to near background levels (1.4-fold increase over pCAT-basic). Mutation of the fp3 NFI-binding site did not significantly affect CAT activity, generating a 9-fold increase over pCAT-basic. CAT activity with the double mutant construct (pCAT-1.8(fp1*3*)) was 2.9-fold higher than with pCAT-basic. Based on these results, we conclude that the fp1-binding site is essential for *B-FABP* promoter activity. In contrast, the fp3 NFI-binding site does not appear to be critical for *B-FABP* promoter activity using this assay.

NFI Isoforms in B-FABP(+) and B-FABP(−) Cell Lines—The differences in the gel shift patterns observed with T98 and U251 nuclear extracts suggest differences in the NFI isoforms expressed in these cells. We tested 8 additional malignant glioma lines, four positive for B-FABP and four negative for B-FABP, to see if there was a correlation between gel shift patterns and B-FABP expression. The four B-FABP(−) lines (A172, CLA, M021, and U87) all gave rise to one or two major complexes with a slow migration rate, similar to the pattern obtained with T98 (Fig. 8). Nuclear extracts from 4/5 B-FABP(+) lines (M049, M103, U373, and U251) generated

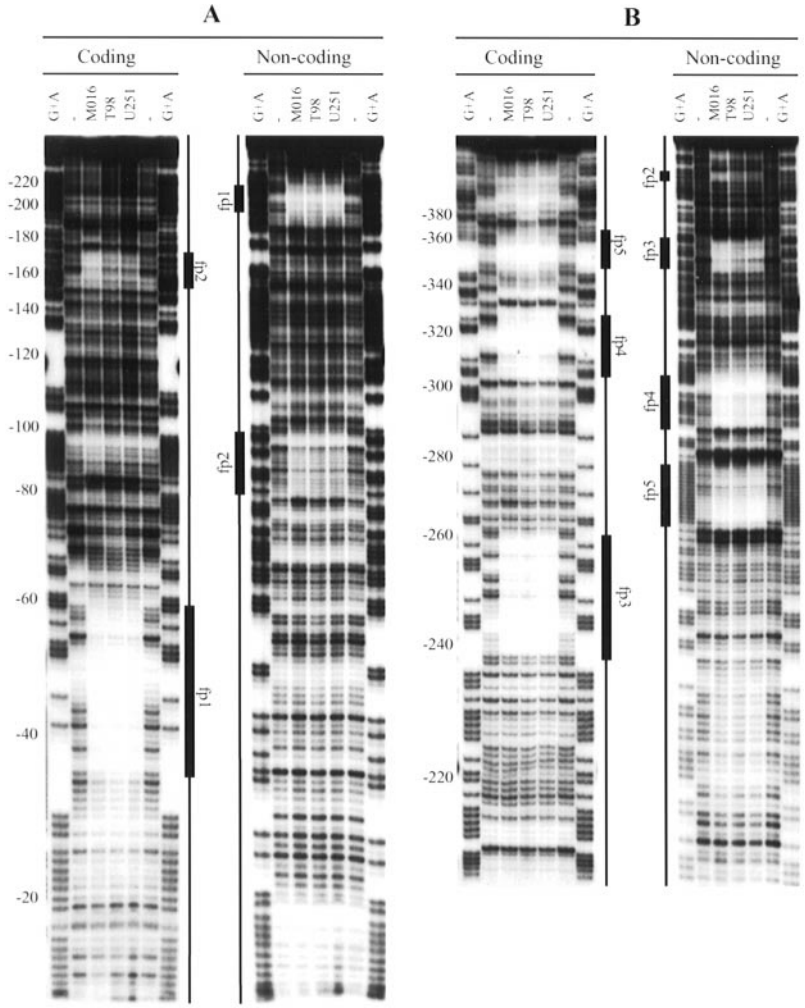

FIG. 2. **DNase I footprinting of the *B-FABP* promoter region.** *A*, a DNA fragment spanning the −13 to −240-bp region of the *B-FABP* promoter (probe 1) was labeled at one end on either the coding or non-coding strand, incubated with T98, M016, or U251 nuclear extracts, digested with DNase I, and run on a 8% denaturing polyacrylamide gel. No nuclear extracts were added to lanes marked −. The G + A lanes represent the purine sequence of probe DNAs. Footprints (*fp*) are indicated by the *filled rectangles*. *B*, DNase I footprint analysis of the −138 to −418-bp region (probe 2).

```
GTCTGGCATTTCAGTGGTTTTCTTTAAGGGGGGTCCTCATTTGTGACCAG   -401

CTTTGTCATTAACGGAAATCAATCTGAATGCCCCATTGTGCATCTTTTTT   -351
fp5                                  fp4
CTTTCCTTGCAGTCTGAGATTGCCTTTGCCAAGTTTTTTCTCACCGAACC   -301

TGAAAGCCCTTCTCTCATTTTCCCGTTCCCTGCCTCCAGCCCCATTGAAT   -251
 fp3
CCCTGCCGAGCTTTCTCAGGCATAAGGGCTGTAGTGTGAGGATTGGGAGG   -201
                                     fp2
AACTCGACCTACTCCGCTAACCCAGTGGCCTGAGCCAATCACAAAGAGGA   -151

TTGGAGCCTCACTCGAGCGCTCCTTCCCTTCTCCTCTCTCTGTGACAGCC   -101

TCTTGGAAAGAGGGACACTGGAGGGGTGTGTTTGCAATTTAAATCACTGG    -51
  fp1
ATTTTTGCCCACCCTCTTTCCAAATAAGAAGGCAGGAGCTGCTTGCTGAG     -1

GTGTAAAGGGTCTTCTGAGCTGCAGTGGCAATTAGACCAGAAGATCCCCG    +50

CTCCTGTCTCTAAAGAGGGGAAAGGGCAAGGATGGTGGAGGCTTTCTGTG   +100
```

FIG. 3. **Summary of footprint results.** The sequence of the +100 to −450-bp *B-FABP* region is shown, indicating the location of the five DNA-binding sites identified by DNase I footprinting. The transcription start site is at position +1. The putative TATA box is *underlined* (from −22 to −28 bp). The sequence in *bold* represents the 5′ end of exon I and the start methionine is *underlined*.

multiple complexes with faster migration rates than those observed with the B-FABP(−) lines. The M016 gel shift pattern varied with different nuclear extract preparations, often appearing as a hybrid of the two patterns, suggesting that this line may include a mixture of B-FABP(−) and B-FABP(+) cells. These results indicate that there is a correlation between B-FABP expression in malignant glioma cells and gel shift patterns, likely reflecting the presence of different forms of NFI in B-FABP(+) and B-FABP(−) cells.

The different migration rates of the NFI protein-DNA complexes in B-FABP(+) and B-FABP(−) lines could be due to differential expression of the *NFI* genes in malignant glioma lines, alternative gene products from a single gene and/or post-translational modification of the NFI protein. NFI protein expression in malignant glioma lines was analyzed by Western blotting using anti-NFI antibody. Although raised against NFI-C, this anti-NFI antibody cross-reacts with the NFI proteins produced from all four NFI genes (28). Two sets of bands, migrating at approximately 50 and 60 kDa, were observed in malignant glioma lines, in agreement with the reported molecular masses of known NFI family members, which range from 52 to 66 kDa (29). The most obvious difference between B-FABP(+) and B-FABP(−) lines was the ratio of the 50- and 60-kDa bands: in B-FABP(+) cells, the 50-kDa bands were predominant with relatively minor amounts of the 60-kDa bands, while in B-FABP(−) cells, the ratio of 50 to 60 kDa bands was approximately equal (Fig. 9*A*). These results provide further evidence that B-FABP(+) and B-FABP(−) cell lines express distinctive subsets of NFI proteins or isoforms.

Differential Phosphorylation of NFI in Malignant Glioma Lines—Phosphorylation of NFI has been shown to modulate its transcriptional activity (30, 31). We therefore examined whether NFI was phosphorylated in our malignant glioma lines. Nuclear extracts from U251 and T98 were treated with

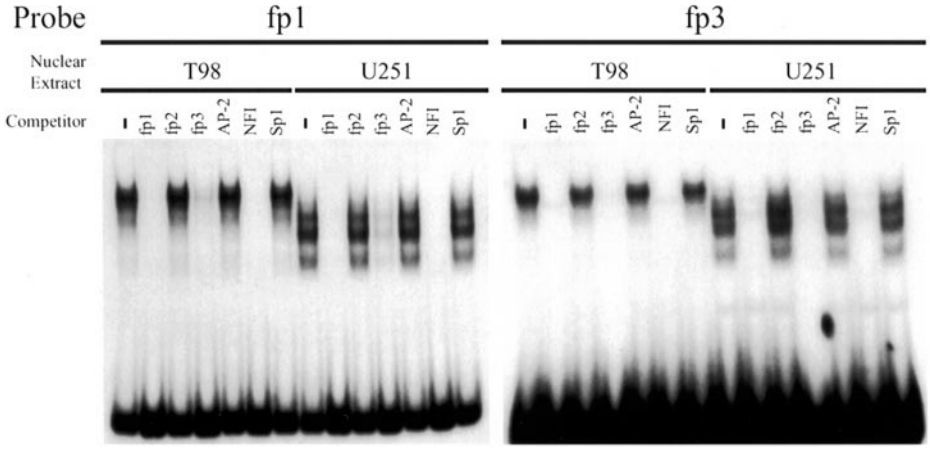

FIG. 4. **Binding of NFI to fp1 and fp3.** Gel shift assays were carried out with radiolabeled fp1 or fp3 double-stranded oligonucleotides and T98 or U251 nuclear extracts. DNA binding reactions were electrophoresed through a 6% polyacrylamide gel in 0.5 × TBE to separate unbound (free) DNA and DNA-protein complexes. Where indicated, a 100-fold excess of unlabeled competitor oligonucleotides were added to the DNA binding reaction.

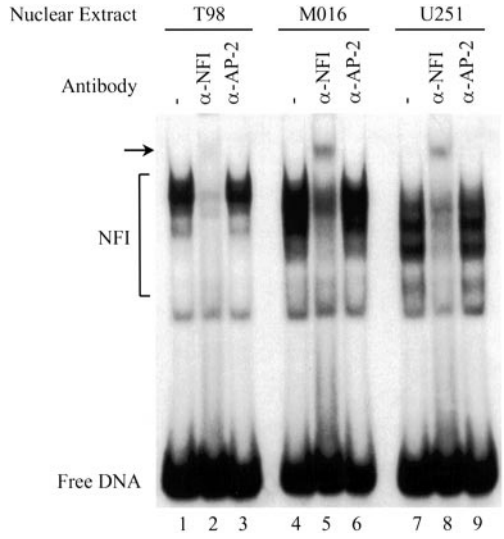

FIG. 5. **Supershifting of fp1 DNA-protein complexes with anti-NFI antibody.** Four μg of T98, M016, or U251 nuclear extract was incubated with anti-NFI antibody (*α-NFI*), anti-AP-2 antibody (*α-AP-2*), or no antibody (−) prior to addition of radiolabeled fp1 oligonucleotide probe and gel electrophoresis. Bands corresponding to unbound (*free*) DNA and NFI-DNA complexes (NFI) are indicated. The *arrow* shows the supershifted complex observed with T98 (weak band), M016 and U251 nuclear extracts in the presence of anti-NFI antibody.

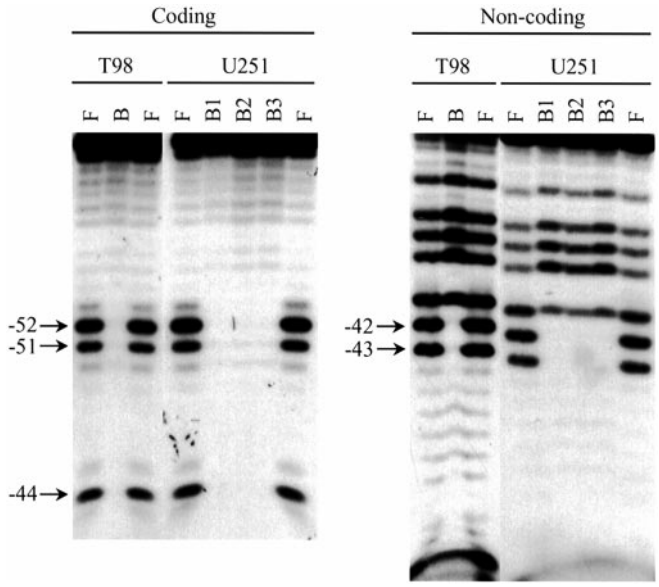

FIG. 6. **Methylation interference assay of fp1 NFI-binding site.** Fp1 oligonucleotide probes radiolabeled on either the coding or non-coding strand were partially methylated with dimethyl sulfate prior to carrying out the gel shift assay. DNA isolated from free (*F*) and NFI-bound (*B*) bands was cleaved with piperidine and run on a 12% denaturing polyacrylamide gel. Guanosine residues that, when methylated, interfere with DNA-protein interaction are indicated by the *arrows*. *B1, B2*, and *B3* represent the three main complexes obtained with U251 extracts.

PAP and analyzed by Western blotting using anti-NFI antibody. The NFI proteins expressed in both U251 and T98 were converted to faster migrating species with PAP treatment (Fig. 9*B*). The proteins migrating at ~60 kDa, predominant in T98, were almost completely converted to faster migrating forms. The slower migrating component of the bands at ~50 kDa also underwent an increase in mobility with phosphatase treatment. The migration pattern of T98 and U251 NFI proteins appeared virtually identical when nuclear extracts were incubated with 0.5 unit of PAP (compare *lanes 4* and *10*). Addition of sodium orthophosphate, a phosphatase inhibitor, resulted in complete inhibition of dephosphorylation at low concentrations of PAP and partial inhibition at high concentrations of PAP. These results indicate that a major difference in the NFI isoforms expressed in U251 and T98 is their phosphorylation state, with T98 NFI isoforms being hyperphosphorylated compared with U251 isoforms.

The gel shift assay was carried out using labeled fp1 oligonucleotide and PAP-treated and -untreated nuclear extracts from T98 and U251. Increasing amounts of PAP resulted in a stepwise increase in the migration rate of NFI-DNA complexes, culminating in the appearance of a single major band where only a weak signal was previously obtained (indicated by the *arrow* in Fig. 10). These results provide further evidence that the NFI isoforms present in T98 are hyperphosphorylated compared with the U251 isoforms.

Analysis of Endogenous Phosphatase Activity in Malignant Glioma Lines—When we prepared T98 and U251 nuclear extracts in phosphate-free buffer, we noticed that U251 nuclear extracts contained a phosphatase activity capable of dephosphorylating NFI that was absent from T98 extracts. As shown in Fig. 11, incubation of these U251 nuclear extracts at 30 °C for 30 min prior to carrying out the gel shift assay resulted in complete dephosphorylation of NFI (*lane 3*). In contrast, no dephosphorylation activity was observed with T98 nuclear ex-

fp1	TTA AAT CAC TGG ATT TTT GCC CAC C A GTG ACC TAA AAA CGG GTG GGA GAA
fp1*	TTA AAT CAC T**AA** ATT TTT GCC CAC C A GTG A**TT** TAA AAA CGG GTG GGA GAA
fp2	GGC CTG AGC CAA TCA CAA AG G GAC TCG GTT AGT GTT TC
fp3	CCC ATT GAA TCC CTG CCG AGC TTT GGG TAA CTT AGG GAC GGC TCG AAA G
fp3*	AGC CCC AT**A** **A**AA TCC CTG CCG AG GGG TA**T** **T**TT AGG GAC GGC TCG AA

SCHEME 1.

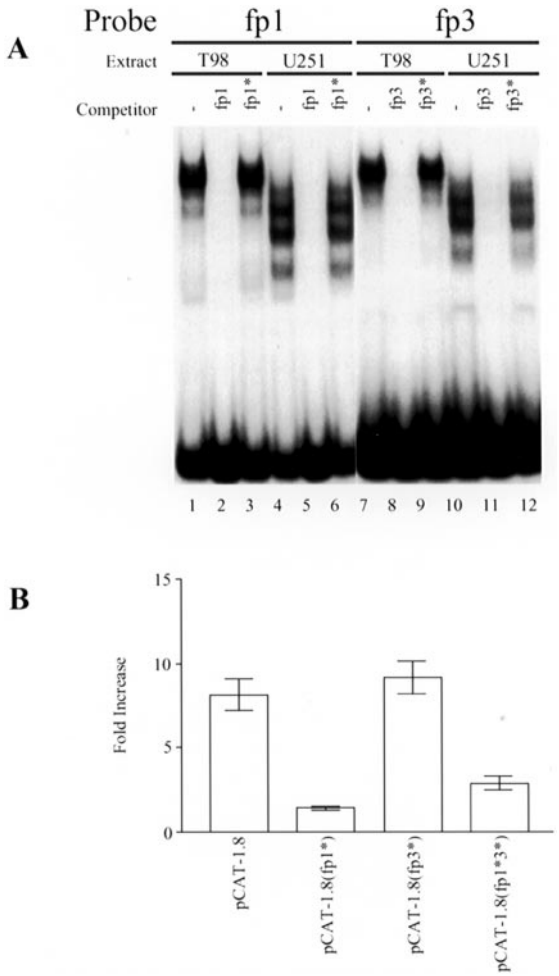

FIG. 7. **Site-directed mutagenesis of fp1 and fp3 NFI-binding sites.** Mutated fp1*- and fp3*-binding sites were tested for NFI binding and for regulatory activity. *A,* gel shift assays with a 100-fold × excess of either fp1* or fp3* failed to compete with wild-type fp1 and fp3 for NFI binding using both U251 and T98 nuclear extracts. *B,* B-FABP-CAT constructs containing mutated fp1*, mutated fp3*, and mutated fp1*fp3* in the context of pCAT-1.8 were transfected into U251 cells. The fold increase in CAT activity represents the average of at least four independent experiments. All values were corrected for transfection efficiency using Hirt DNA. The *error bars* indicate the standard deviation.

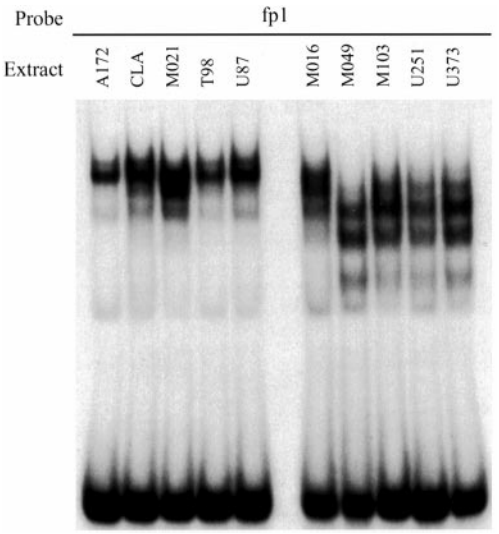

FIG. 8. **Gel shift patterns in B-FABP(+) and B-FABP(−) malignant glioma lines.** The gel shift assay was carried out using fp1 oligonucleotide and nuclear extracts prepared from five B-FABP(−) cell lines (A172, CLA, M021, T98, and U87) and five B-FABP(+) lines (M016, M049, M103, U251, and U373).

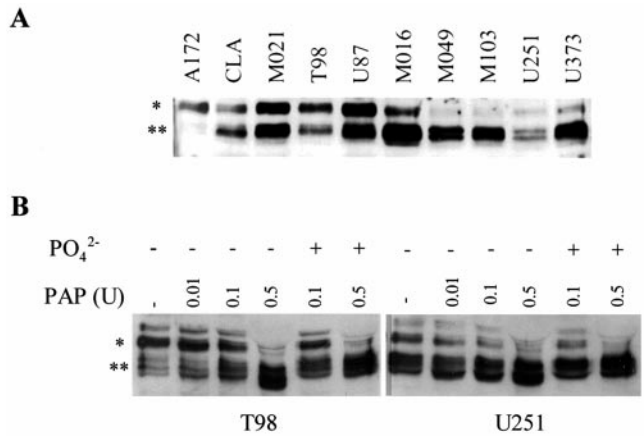

FIG. 9. **Western analysis of NFI in malignant glioma lines.** *A,* nuclear extracts from the 10 malignant glioma listed in Fig. 8 were run on an 8% SDS-polyacrylamide electrophoresis gel and electroblotted to a nitrocellulose filter. *B,* nuclear extracts from T98 and U251 were treated with increasing concentrations of PAP (*U*, units) in the presence or absence of 100 mM NaH_2PO_4, pH 6.5, for 20 min at 30 °C and run on a 10% SDS-polyacrylamide electrophoresis gel. The filters were incubated with anti-NFI antibody and the signal detected using the ECL system. The ~60-kDa bands are indicated by the *single asterisk* while the ~50-kDa bands are indicated by the *double asterisks*.

tracts (*lane 1*). This phosphatase activity was inhibited by the addition of 50 mM PO_4^{2-} (compare *lanes 3* and *4*). Furthermore, incubation of the T98 nuclear extract with an equal amount of U251 nuclear extract resulted in dephosphorylation of the hyperphosphorylated T98 NFI (compare *lanes 1, 3,* and *5*). Addition of PO_4^{2-} effectively inhibited this activity (*lane 6*). These results indicate that a phosphatase activity, present in B-FABP(+) cells but not in B-FABP(−) cells, may underlie differential NFI phosphorylation in malignant glioma.

DISCUSSION

In a previous study, we showed that the subset of malignant glioma lines that expresses GFAP also expresses B-FABP (9). GFAP is a marker of mature astrocytes and its expression in malignant glioma correlates with a less aggressive phenotype (2). B-FABP is also expressed in cells of the glial lineage although it is found at earlier developmental stages than GFAP, in radial glial cells and immature astrocytes (10, 11). Here, we study the regulation of the *B-FABP* gene in malignant glioma lines in order to understand the molecular mechanism underlying differential expression of B-FABP. We identified two NFI-binding sites located upstream of the *B-FABP* gene, one at −35 to −58 bp, the other at −237 to −260 bp. Our transient trans-

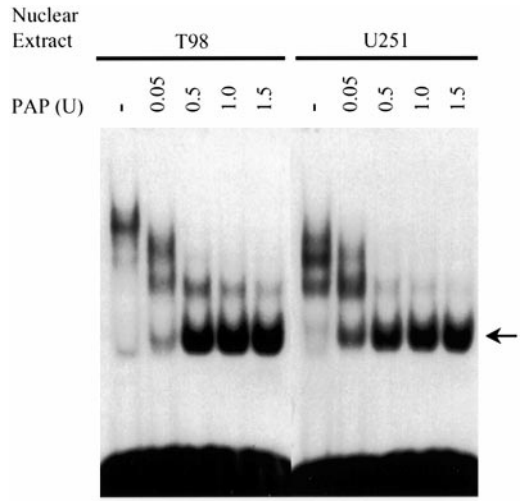

FIG. 10. **Differential phosphorylation of NFI in T98 and U251.** T98 and U251 nuclear extracts (4 μg) were treated with increasing concentrations of PAP (*U*, units) and the gel shift assay carried out with radiolabeled fp1 oligonucleotide. The *arrow* marks the position of the dephosphorylated NFI-fp1 complex.

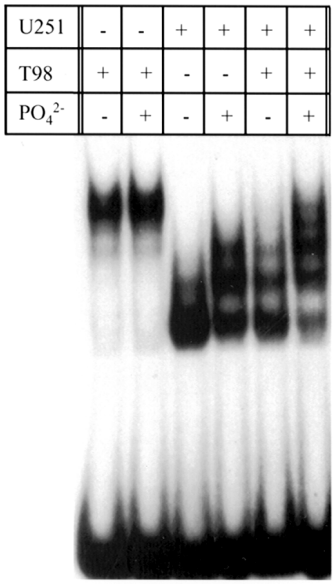

FIG. 11. **Endogenous phosphatase activity in U251.** T98 (*lanes 1* and *2*), U251 (*lanes 3* and *4*), or an equal mixture of T98 and U251 (*lanes 5* and *6*) nuclear extracts in phosphate-free buffer were incubated at 30 °C for 30 min in the absence (*lanes 1, 3*, and *5*) or presence (*lanes 2, 4*, and *6*) of 50 mM K_2PO_4, pH 7.4, prior to the gel shift assay with radiolabeled fp1 oligonucleotide.

fection experiments using the CAT reporter gene indicate that at least 660 bp of 5′-flanking DNA are required for efficient transcription. Mutation of the most proximal NFI-binding site dramatically reduced reporter activity in a B-FABP-expressing malignant glioma line, indicating that this region is critical but not sufficient for *B-FABP* transcription.

Originally identified as a factor involved in adenovirus DNA replication, NFI is now a well characterized transcription factor implicated in the regulation of many cellular genes. The NFI family is encoded by at least four genes: NFI-A, -B, -C, and -X (32–34). Additional diversity within this protein family comes from alternative splicing (34). NFI factors bind to their consensus recognition site 5′-YTGG(A/C)N_5GCCAR-3′ as heterodimers or homodimers (35, 36). NFI proteins are found in a variety of cell types; however, the expression patterns of individual NFIs varies considerably (37). For example, NFI-A is enriched in the cerebellum (38) while NFI-X levels are elevated in fetal glial cells (39). NFI has long been implicated in the regulation of glial cell-specific genes. For example, the regulatory elements of the human JC papovavirus which include at least two active NFI sites are only functional in glial cells (40, 41). One of the best characterized cellular targets for NFI is the glial cell-specific myelin basic protein gene (42, 43). *GFAP* has recently been proposed to be regulated by NFI-A based on the observation that GFAP levels (but not levels of S100, another astrocyte marker) are reduced in *NF1A*−/− mice (44). *B-FABP* represents another example of a gene expressed in glial cells gene (in this case, radial glial cells) regulated by NFI.

Because NFI transcription factors have a wide distribution and all NFI factors recognize the same DNA-binding domain, the basis for cell-specific gene regulation by members of the NFI family has long been a matter of speculation. Recent studies indicate that different forms of NFI have different transactivation capabilities and that heterodimers differ from homodimers in their activation potential (45). Furthermore, NFI proteins generated by alternative splicing are capable of interfering with transcriptional activation (46, 47). For example, Liu *et al*. (47) have isolated an NFI-B splice variant, NFI-B3, that lacks the trans-activation domain and interferes with NFI-mediated transactivation as the result of nonproductive heterodimer formation. On the basis of these observations, we were especially interested in determining whether differential B-FABP expression in malignant glioma was dependent on the types of NFIs expressed in these cells. By Northern blot analysis, we found no clear-cut correlation between B-FABP expression and specific NFI transcripts although there was a general trend toward higher levels of NFI-A and NFI-B mRNA in B-FABP(+) lines compared with B-FABP(−) lines (data not shown).

The most striking differences between B-FABP(+) and B-FABP(−) lines were identified by Western blotting using an anti-NFI antibody that recognizes the different forms of NFI and by gel mobility shift assays. Two sets of bands were observed on Western blots, at ~50 and ~60 kDa. The ratio of 60- to 50-kDa bands was higher in B-FABP(−) lines compared with B-FABP(+) lines. Similarly, gel shift assays with the proximal NFI-binding site produced two distinct patterns: nuclear extracts from B-FABP(+) lines generated multiple bands of relatively high mobility, while nuclear extracts from B-FABP(−) lines produced bands of lower mobility. By treating nuclear extracts with potato acid phosphatase, we found that the basis for the difference in mobility observed in both the Western blots and gel shift assays was the phosphorylation state of NFI. Our results indicate that the NFI factors expressed in B-FABP(−) lines are hyperphosphorylated compared with those expressed in B-FABP(+) lines.

Protein phosphorylation has previously been implicated in the modulation of NFI-mediated transactivation (30, 31, 48). Yang *et al*. (31) have shown that NFI is phosphorylated in actively growing cells and in c-Myc-overexpressing 3T3-L1 cells, whereas it is dephosphorylated in quiescent cells. The phosphorylated forms of NFI present in c-Myc-overexpressing cells transactivated NFI-dependent promoters at a lower rate than the dephosphorylated form. No significant differences in DNA binding affinity were observed between the dephosphorylated and phosphorylated forms of NFI (31). The gel shift pattern that we observed with B-FABP(+) extracts appears to be similar if not identical to the phosphorylated (lower activity) NFI pattern described by Yang *et al*. (31). In agreement with these authors, we found no significant differences in footprint patterns and DNA binding affinity between B-FABP(+) cells expressing phosphorylated NFI and B-FABP(−) cells express-

ing hyperphosphorylated NFI (Figs. 2 and 4, and data not shown). In combination with the data from Yang *et al*. (31), our results suggest a gradation in the transactivation potential of NFI based on its phosphorylation level, with dephosphorylated NFI being most active, moderately phosphorylated NFI (B-FABP(+), U251-like) having intermediate activity and hyperphosphorylated NFI (B-FABP(−), T98-like) being least active. Given the variety of genes responsive to NFI, regulation of its activity by phosphorylation is likely to have global effects on gene expression, with important cellular consequences. These results are especially important in the context of malignant glioma, in that dephosphorylation of NFI in these cells could lead to increased activation of glial-specific genes which, in turn, could lead to increased cellular differentiation properties.

The molecular mechanism(s) underlying NFI phosphorylation has not yet been elucidated. Additional work will be required to identify the kinase(s) and phosphatase(s) involved in NFI phosphorylation. Two kinases, DNA-PK and CDC2, have been reported to phosphorylate NFI proteins *in vitro* (48, 49). Of particular interest is the phosphatase activity identified in B-FABP(+) U251 but not in B-FABP(−) T98. PTEN (MMAC1, TEP1) is a phosphatase that is commonly mutated in malignant glioma tumors and cell lines. Introduction of PTEN in the U87 malignant glioma line results in reduced growth rate and saturation density (50). However, it is unlikely that PTEN is the phosphatase involved in NFI dephosphorylation because: (i) *PTEN* mutations have been reported in both B-FABP(+) and B-FABP(−) malignant glioma lines (51, 52) and (ii) PTEN has a cytosolic location (53).

Our DNA transfection experiments and DNase I footprinting suggest that regulatory elements in addition to NFI are necessary to drive B-FABP expression in malignant glioma lines. Footprints 4 and 5 located upstream of the two NFI-binding sites (300 to 400 bp upstream of the *B-FABP* gene) remain to be characterized. Feng and Heintz (21) have studied the regulation of murine B-FABP using transgenic mice. They have found a radial glial element (RGE) in the −0.3 to −0.8-kb region of the murine *B-FABP* promoter responsible for transcriptional up-regulation in radial glial cells. Two regulatory elements within this region have recently been characterized by Josephson *et al*. (54): a POU-binding site at −362 to −370 bp, and a non-steroid hormone response element at −275 to −286 bp. In the mouse, the POU-binding site is essential for appropriate B-FABP expression in the developing central nervous system while the hormone response element is required to drive wild-type levels of B-FABP expression in the developing telencephalon. Although both sites are conserved in the human *B-FABP* promoter, we did not detect DNA-protein interactions in the corresponding region by DNase I footprint analysis. The reason for these differences is not clear, but it does suggest alternative mechanisms for *B-FABP* gene regulation in human malignant glioma and mouse brain.

In summary, we have shown that the promoter of the human *B-FABP* gene contains two NFI-binding sites and that the site most proximal to the *B-FABP* gene is essential for *B-FABP* transcription. NFI proteins in B-FABP(+) and B-FABP(−) malignant glioma cell lines are differentially phosphorylated, with B-FABP(−) lines producing a hyperphosphorylated and presumably inactive form of NFI. Differential NFI phosphorylation in these lines appears to be due, at least in part, to a phosphatase activity that is specific to B-FABP(+) cells. Given the number of proposed target genes for NFI, activation and deactivation of this transcription factor through phosphorylation will likely have major consequences on gene expression and cellular growth properties. Isolation and characterization of the NFI phosphatase and examining its role in glial cell differentiation will be the subject of future investigations.

Acknowledgments—We thank Dr. Rufus Day III for supplying the cell lines used in this study and Dr. Naoko Tanese for the anti-NFI antibody. We also thank Dr. Xuejun Sun and Sachin Katyal for help with the preparation of the figures.

REFERENCES

1. Eng, L. F., and Rubinstein, L. J. (1978) *J. Histochem. Cytochem.* **26,** 513–522
2. Russell, D. S., and Rubinstein, L. J. (1989) *Pathology of Tumours of the Nervous System,* Williams & Wilkins, London
3. van der Meulen, J. D., Houthoff, H. J., and Ebels, E. J. (1978) *Neuropathol. Appl. Neurobiol.* **4,** 177–190
4. Velasco, M. E., Dahl, D., Roessmann, U., and Gambetti, P. (1980) *Cancer* **45,** 484–494
5. Murphy, K. G., Hatton, J. D., and Sang, H. (1998) *J. Neurosurg.* **89,** 997–1006
6. Rutka, J. T., and Smith, S. L. (1993) *Cancer Res.* **53,** 3624–3631
7. Toda, M., Miura, M., Asou, H., Sugiyama, I., Kawase, T., and Uyemura, K. (1999) *Neurochem. Res.* **24,** 339–343
8. Rutka, J. T., Hubbard, S. L., Fukuyama, K., Matsuzawa, K., Dirks, P. B., and Becker, L. E. (1994) *Cancer Res.* **54,** 3267–3272
9. Godbout, R., Bisgrove, D. A., Shkolny, D., and Day, R. S., III (1998) *Oncogene* **16,** 1955–1962
10. Feng, L., Hatten, M. E., and Heintz, N. (1994) *Neuron* **12,** 895–908
11. Kurtz, A., Zimmer, A., Schnütgen, F., Brüning, F., Spener, F., and Müller, T. (1994) *Development* **120,** 2637–2649
12. Hatten, M. E. (1999) *Annu. Rev. Neurosci.* **22,** 511–539
13. Schmechel, D., and Rakic, P. (1979) *Anat. Embryol.* **156,** 115–152
14. Hirt, B. (1967) *J. Mol. Biol.* **26,** 365–369
15. Hemsley, A., Arnheim, N., Toney, M. D., Cortopassi, G., and Galas, D. J. (1989) *Nucleic Acids Res.* **17,** 6545–6551
16. Belikov, S., and Wieslander, L. (1995) *Nucleic Acids Res.* **23,** 310
17. Roy, R. J., Gosselin, P., and Guérin, S. L. (1991) *BioTechniques* **11,** 770–777
18. Jones, K. A., Yamamoto, K. R., and Tjian, R. (1985) *Cell* **42,** 559–572
19. O'Brien, R. M., Noisin, E. L., Suwanichkul, A., Yamasaki, T., Lucas, P. C., Wang, J.-C., Powell, D. R., and Granner, D. K. (1995) *Mol. Cell. Biol.* **15,** 1747–1758
20. Garabedian, M. J., LaBaer, J., Liu, W.-H., and Thomas, J. R. (1993) in *Gene Transcription: A Practical Approach* (Hames, B. D., and Higgins, S. J., eds) pp. 243–291, IRL Press, Oxford, United Kingdom
21. Feng, L., and Heintz, N. (1995) *Development* **121,** 1719–1730
22. Quandt, K., Frech, K., Karas, H., Wingender, E., and Werner, T. (1995) *Nucleic Acids Res.* **23,** 4878–4884
23. Gronostajski, R. M., Adhya, S., Nagata, R. A., Guggenheimer, A., and Hurwitz, J. (1985) *Mol. Cell. Biol.* **5,** 964–971
24. Jones, K. A., Kadonaga, J. T., Rosenfeld, P. J., Kelly, T. J., and Tjian, R. (1987) *Cell* **48,** 79–89
25. Nagata, K., Guggenheimer, R. A., and Hurwitz, J. (1983) *Proc. Natl. Acad. Sci. U. S. A.* **80,** 6177–6181
26. De Vries, E., van Driel, W., van der Heuvel, S. J. L., and van der Vliet, P. C. (1987) *EMBO J.* **6,** 161–168
27. Raymondjean, M., Cereghini, S., and Yaniv, M. (1988) *Proc. Natl. Acad. Sci. U. S. A.* **85,** 757–761
28. Ortiz, L., Aza-Blanc, P., Zannini, M., Cato, A. C. B., and Santisteban, P. (1999) *J. Biol. Chem.* **274,** 15213–15221
29. Rosenfeld, P. J., and Kelly, T. J. (1986) *J. Biol. Chem.* **261,** 1398–1408
30. Cooke, D. W., and Lane, M. D. (1999) *J. Biol. Chem.* **274,** 12917–12924
31. Yang, B., Gilbert, J. D., and Freytag, S. O. (1993) *Mol. Cell. Biol.* **13,** 3093–3102
32. Qian, F., Kruse, U., Lichter, P., and Sippel, A. E. (1995) *Genomics* **28,** 66–73
33. Rupp, R. A. W., Kruse, U., Multhaup, G., Göbel, U., Beyreuther, K., and Sippel, A. E. (1990) *Nucleic Acids Res.* **18,** 2607–2616
34. Santoro, C., Mermod, N., Andrews, P. C., and Tjian, R. (1988) *Nature* **334,** 218–224
35. Roulet, E., Bucher, P., Schneider, R., Wingender, E., Dusserre, Y., Werner, T., and Mermod, N. (2000) *J. Mol. Biol.* **297,** 833–848
36. Kruse, U., and Sippel, A. E. (1994) *FEBS Lett.* **348,** 46–50
37. Chaudhry, A. Z., Lyons, G. E., and Gronostajski, R. M. (1997) *Dev. Dyn.* **208,** 313–325
38. Krebs, C. J., Dey, B., and Kumar, G. (1996) *J. Neurochem.* **66,** 1354–1361
39. Sumner, C., Shinohara, T., Durham, L., Traub, R., Major, E. O., and Amemiya, K. (1996) *J. Neurovirol.* **2,** 87–100
40. Amemiya, K., Traub, R., Durham, L., and Major, E. O. (1992) *J. Biol. Chem.* **267,** 14204–14211
41. Kumar, K. U., Pater, A., and Pater, M. M. (1993) *J. Virol.* **67,** 572–576
42. Inoue, T., Tamura, T., Furuichi, T., and Mikoshiba, K. (1990) *J. Biol. Chem.* **265,** 19065–19070
43. Verity, A. N., and Campagnoni, A. T. (1988) *J. Neurosci. Res.* **21,** 238–248
44. das Neves, L., Duchala, C. S., Godinho, F., Haxhiu, M. A., Colmenares, C., Macklin, W. B., Campbell, C. E., Butz, K. G., and Gronostajski, R. M. (1999) *Proc. Natl. Acad. Sci. U. S. A.* **96,** 11946–11951
45. Chaudhry, A. Z., Vitullo, A. D., and Gronostajski, R. M. (1998) *J. Biol. Chem.* **273,** 18538–18546
46. Apt, D., Liu, Y., and Bernard, H.-U. (1994) *Nucleic Acids Res.* **22,** 3825–3833
47. Liu, Y., Bernard, H., and Apt, D. (1997) *J. Biol. Chem.* **272,** 10739–10745
48. Jackson, S. P., MacDonald, J. J., Lees-Miller, S., and Tjian, R. (1990) *Cell* **63,** 155–165
49. Kawamura, H., Nagata, K., Masamune, Y., and Nakanishi, Y. (1993) *Biochem. Biophys. Res. Commun.* **192,** 1424–1431
50. Morimoto, A. M., Berson, A. E., Fujii, G. H., Teng, D. H., Tavtigian, S. V., Bookstein, R., Steck, P. A., and Bolen, J. B. (1999) *Oncogene* **18,** 1261–1266

51. Li, J., Yen, C., Liaw, D., Podsypanina, K., Bose, S., Wang, S. I., Puc, J., Miliaresis, C., Rodgers, L., McCombie, R., Bigner, S. H., Giovanella, B. C., Ittmann, M., Tycko, B., Hibshoosh, H., Wigler, M. H., and Parsons, R. (1997) *Science* **275,** 1943–1947
52. Steck, P. A., Pershouse, M. A., Jasser, S. A., Yung, W. K. A., Lin, H., Ligon, A. H., Langford, L. A., Baumgard, M. L., Hattier, T., Davis, T., Frye, C., Hu, R., Swedlund, B., Teng, D. H. F., and Tavtigian, S. V. (1997) *Nat. Genet.* **15,** 356–362
53. Gray, I. C., Phillips, S. M. A., Hamilton, J. A., Gray, N. E., Watson, G. J., Spurr, N. K., and Snary, D. (1998) *Br. J. Cancer* **78,** 1296–1300
54. Josephson, R., Müller, T., Pickel, J., Okabe, S., Reynolds, K., Turner, P. A., Zimmer, A., and McKay, R. D. G. (1998) *Development* **125,** 3087–3100